Hindawi Publishing Corporation
Journal of Biomedicine and Biotechnology
Volume 2007, Article ID 94740, 9 pages
doi:10.1155/2007/94740

Research Article

Superparamagnetic Iron Oxide Nanoparticles Coated with Galactose-Carrying Polymer for Hepatocyte Targeting

Mi Kyong Yoo,[1] In Yong Kim,[1] Eun Mi Kim,[2] Hwan-Jeong Jeong,[2] Chang-Moon Lee,[2] Yong Yeon Jeong,[3] Toshihiro Akaike,[4] and Chong Su Cho[1]

[1] *School of Agricultural Biotechnology, Seoul National University, Seoul 151-921, South Korea*
[2] *Department of Nuclear Medicine, Chonbuk National University School of Medicine, Jeonju 561-712, South Korea*
[3] *Department of Diagnostic Radiology, Chonnam National University Medical School, Gwangju 501-746, South Korea*
[4] *Department of Biomolecular Engineering, Tokyo Institute of Technology, Yokohama 226-8501, Japan*

Correspondence should be addressed to Chong Su Cho, chocs@plaza.snu.ac.kr

Received 2 April 2007; Accepted 24 December 2007

Recommended by Marek Osinski

Our goal is to develop the functionalized superparamagnetic iron oxide nanoparticles (SPIONs) demonstrating the capacities to be delivered in liver specifically and to be dispersed in physiological environment stably. For this purpose, SPIONs were coated with polyvinylbenzyl- *O*-β-D-galactopyranosyl-D-gluconamide (PVLA) having galactose moieties to be recognized by asialoglycoprotein receptors (ASGP-R) on hepatocytes. For use as a control, we also prepared SPIONs coordinated with 2-pyrrolidone. The sizes, size distribution, structure, and coating of the nanoparticles were characterized by transmission electron microscopy (TEM), electrophoretic light scattering spectrophotometer (ELS), X-ray diffractometer (XRD), and Fourier transform infrared (FT-IR), respectively. Intracellular uptake of the PVLA-coated SPIONs was visualized by confocal laser scanning microscopy, and their hepatocyte-specific delivery was also investigated through magnetic resonance (MR) images of rat liver. MRI experimental results indicated that the PVLA-coated SPIONs possess the more specific accumulation property in liver compared with control, which suggests their potential utility as liver-targeting MRI contrast agent.

1. INTRODUCTION

In the last decade, many investigations with several types of iron oxides have been carried out in the field of nanosized magnetic particles (mostly, magnetite (Fe_3O_4) or maghemite (γ-Fe_2O_3) single domains of about 5∼20 nm in diameter) [1]. These iron oxide particles of nanometer size present superparamagnetic property and are ideal for magnetic resonance imaging (MRI) contrast agent by enhancement of proton relaxation in the tissue microenvironment [2–4].

For the MRI application, these SPIONs must have high magnetization values, stability in physiological environment, and size smaller than 20 nm with overall narrow particle size distribution so that the particles have uniform physical and chemical properties [5]. However, the iron oxide magnetic nanoparticles have several problems such as aggregation in water, chemical instability in air, biodegradability in physiological environment, and toxicity, which limit their use to the medical diagnostic agent. Ferrofluids are colloidal suspensions of magnetic nanoparticles, forming magnetizable fluids that remain liquid in the most intense magnetic fields [6]. Even though the stability of the ferrofluid is of utmost importance for its biomedical applications, the nanoparticles in colloidal suspension are likely to agglomerate and form large cluster due to hydrophobic interactions between the magnetic iron oxide particles with a large hydrophobic surface area to volume ratio [1]. These problems of naked iron oxide nanoparticles have been overcome by coating the surface of magnetic particles with synthetic polymers such as polyethylene glycol (PEG) [7], polyvinyl alchol (PVA) [8], polyvinyl pyrrolidone (PVP) [9], and natural polymers like dextran [10], chitosan [11], and pullulan [12]. However, the nanoparticles coated with the above-mentioned polymers were nonspecifically accumulated into tissues and organs, resulting in the poor availability in the imaging of specific tissues and organs [13, 14]. Therefore, targeted delivery of MRI contrast agent is a highly desirable strategy for enhancing efficiency and reducing unintended side-effects and toxicity

[14, 15]. One strategy to realize efficient and specific delivery of SPIONs is to modify the nanoparticle surface with a ligand that is efficiently taken up by target cells via receptor-mediated endocytosis [16].

In this work, our prime aim is to achieve hepatocytes-specific delivery of SPIONs by coating with galactose-carrying polymer for liver imaging as well as to enhance their functions in vivo containing the stabilization of magnetic fluid suspension.

PVLA, that is, a galactose-carrying polymer, has an amphiphilic structural unit composed of hydrophilic oligosaccharide side chains covalently bound to a hydrophobic polystyrene backbone. The binding profile of the carbohydrating ligands with cell surface receptors has been well characterized for ASGP-R on hepatic parenchyma1 cells [17–19]. The ASGP-R recognizes galactose or *N*-acetylgalactosamine residues of desialylated glycoproteins and brings into the hepatocytes through endocytotic process as a ligand-receptor complex [20, 21]. Further, the amphiphilic structure of PVLA allows it to serve as an emulsifier. Maruyama et al. reported that the nanoparticles prepared using the PLVA as an emulsifier were hardly aggregated during storage and centrifugal treatment [22]. Therefore, such capabilities of PVLA will open the door to the design and synthesis of MRI contrast agent that can be accumulated specifically on liver without aggregation in physiological medium.

In this study, PVLA-coated SPIONs were prepared by traditional coprecipitation method, followed by a thermochemical treatment and postcoating with PVLA solution. Various characterization techniques have been applied to obtain information about the sizes, structure, and coating of the nanoparticles. Intracellular trafficking of the PVLA-coated SPIONs was visualized by confocal laser scanning microscopy and their hepatocyte-specific delivery was also investigated through MR images of rat liver.

2. MATERIALS AND METHODS

2.1. Materials

Ferric chloride hexahydrate ($FeCl_3 \cdot 6H_2O > 97\%$) and ferrous chloride tetrahydrate ($FeCl_2 \cdot 4H_2O > 99\%$) were purchased from Sigma-Aldrich (St. Luois, Miss, USA). PVLA ($MW = 5 \times 10^4$) was prepared by the same method previously reported [23]. The chemical structure of PVLA is shown in Figure 1. Fluorescence labeling of PVLA was performed similar to the method previously described [22]. All other chemicals were of analytical reagent grade and were used without further purification.

2.2. Iron oxide nanoparticles

PVLA-coated SPIONs were prepared by alkaline coprecipitation of ferric and ferrous chlorides in aqueous solution [24, 25]. $FeCl_3 \cdot 6H_2O$ (3.255 g, 12.04 mmol) and $FeCl_2 \cdot 4H_2O$ (1.197 g, 6.02 mmol) were dissolved in 70 mL of deoxygenated water, respectively. In a typical experimental procedure, the solutions were mixed and precipitated by adding 7 mL of NH_4OH solution (28–30%) while stirring vigorously. The black precipitate which immediately formed was washed several times with ultrapure water until the pH decreased from 10 to 7. After sedimenting the precipitate with a permanent magnet, the supernatant was removed by decantation. Then 20 mL of 2 M HNO_3 was added to the black sediment and the mixture was stirred for 5 minutes. After adding 30 mL of 0.35 M $Fe(NO_3)_3$ to the mixture, it was refluxed for 1 hour under nitrogen gas. During this step, the initial black slurry turned brown. The system was allowed to cool to room temperature, the remaining liquid was discarded, and 50 mL of ultrapure water was added to the slurry which immediately dispersed. The brown suspension was dialyzed for 2 days against 0.01 M nitric acid, and stored at 4°C. In a final step, the obtained product was mixed with solution of PVLA to obtain SPIONs coated with PVLA. For biological investigations, the pH was adjusted to 7 using aqueous ammonia [8]. The content of SPIONs in the ferrofluid was determined by dry weight analysis [26].

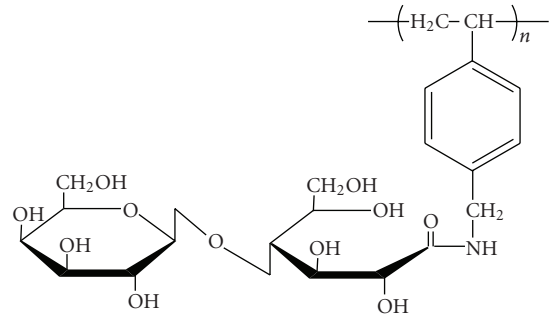

Figure 1: Chemical structure of PVLA, β-galactose-carrying polymer.

For use as a control, 2-pyrrolidone-coated SPIONs were prepared through thermal decomposition of ferric triacetylacetonate ($Fe(acac)_3$) in hot organic solvent, 2-pyrrolidone, by following previously developed method [27]. However, 2-pyrrolidone not only serves as a media for high-temperature reaction, but also involves surface coordination which renders the magnetic nanoparticles water-soluble and colloidal solution stable [27]. Before the sample was withdrawn, the dispersed solution was sonicated for 5 minutes to obtain the better particle dispersion.

2.3. Characterization

Fourier transform infrared (FT-IR) spectra were recorded in the transmission mode on a Nicolet Magna 550 series II spectrometer (Midac, Atlanta, Ga, USA). The transparent films for SPIONs, PVLA, and PVLA-coated SPIONs were prepared by casting each solution on silicon wafer and followed by drying at room temperature.

The size of SPIONs was assessed using an electrophoretic light scattering spectrophotometer (ELS 8000, Otsuka Electronics, Osaka, Japan) with 90° and 20° scattering angles at 25°C. The volume of the samples was 4 mL containing a final concentration of 1 mg/mL in distilled water.

The average particle size and morphology of SPIONs were observed by transmission electron microscopy (TEM)

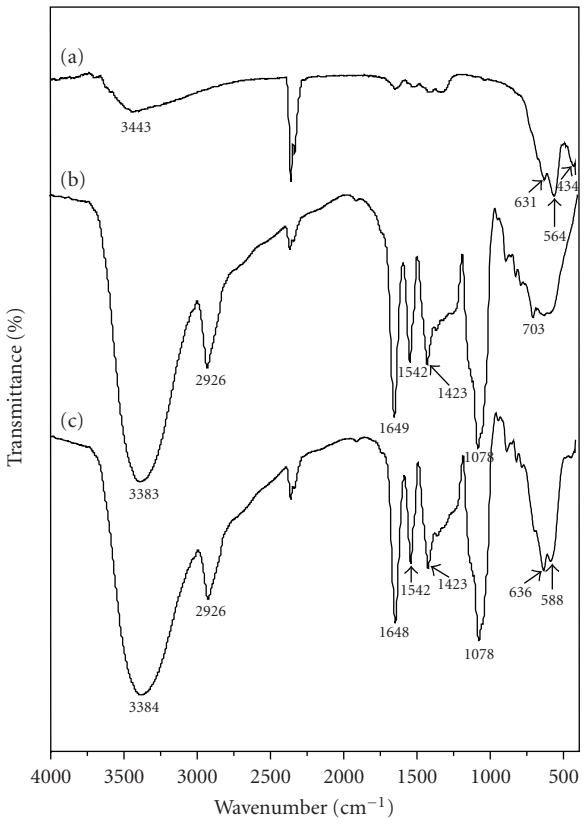

Figure 2: FTIR spectra of SPIONs (a), PVLA (b), and PVLA-coated SPIONs (c).

using a JEOL Model JEM 1010 at 80 kV. For sample preparation, a diluted drop of SPIONs suspension was placed on a carbon-coated copper grid. The grid was allowed in air to dry further for 15 minutes and was then examined with the electron microscope.

To investigate the nanocrystallinity of SPIONs, X-ray diffraction (XRD) data were collected on an X-ray diffractometer (Bruker-AXS GmbH D8 Advance, Karlsruhe, Germany) equipped with a rotating anode, Sol-X energy dispersive detector, and Cu-Kα radiation source ($\lambda = 0.1542$ nm).

2.4. Hepatocyte isolation and culture

Hepatocytes were prepared by noncirculation perfusion of male ICR mouse liver with a two-step collagenase perfusion technique of Seglen [28]. Briefly, the male ICR mice (5–7 weeks of age) employed in this study were purchased from Jungang Lab. Animal, Inc. (Seoul, Korea). The liver was perfused by 0.5 mM of ethylene glycol-bis[β-amino ethyl ether]-*N*,*N*,*N*′′,*N*′′-tetraacetic acid (EGTA) in Hanks' balanced salt solution (HBSS) without $CaCl_2$ and 5×10^{-3}% (wt./wt.) collagenase in HBSS with $CaCl_2$ (5 mM) through a disposable needle (25G-1) aligned along the inferior vena cava. The collagenase-perfused liver was dissected, suspended in HBSS, and filtered through cheesecloth and 100-μm nylon membrane to remove connective tissue debris and cell clumps. Hepatocytes were purified by a density-gradient centrifugation (50 g force, 10 minutes) using 45% Percoll solution (Pharmacia, Piscataway, NJ, USA) at 4°C. Cell viability measured by trypan blue exclusion was more than 90%.

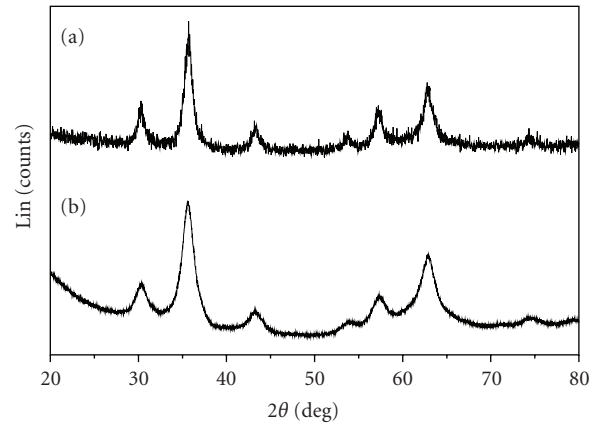

Figure 3: X-ray diffraction patterns of 2-pyrrolidone-coated SPIONs (a), PVLA-coated SPIONs (b).

Isolated hepatocytes were suspended in a serum-free Williams' E (WE) medium (Gibco BRL, NY, USA) containing 50 μg/mL penicillin and 50 μg/mL streptomycin.

2.5. Observation of phase contrast, fluorescence, and confocal laser scanning micrographs

The isolated hepatocytes were plated on collagen-coated glass cover slips in 12-well plates (Iwaki Glass Co., Tokyo, Japan) at 1×10^5 cells per well. The hepatocytes were incubated at 37°C for 2 hours. Then, the old medium was removed and WE medium containing FITC-PVLA-coated SPIONs (1 mg/mL) was added to cells. After 15-, 30-, and 60-minute incubation, cells were rinsed twice with 0.1 M PBS. The coverslips were enclosed in 1 mL of glycerol and visualized by confocal laser scanning microscope (Micro Systems LSM 410, Carl Zeiss, Germany). Gallery mode of optical sections was used for checking internalization of complexes into cells [29, 30].

2.6. In vivo MR image

For all rats, liver MR images were taken prior and 1 hour after injection of contrast agents. PVLA-coated SPIONs and pyrrolidone-coated SPIONs were intravenously injected through the tail vein. Rats (SD, female, 6 weeks) were anesthetized with the use of a general inhalation anesthesia (1.5% isoflurane in a 1 : 2 mixture of O_2/N_2) during MR examination. MR imagings were performed with a 1.5 T MR scanner (GE Signa Exite Twin-speed, GE Health Care, Milwaukee, Wiss, USA) using an animal coil (4.3 cm Quadrature volume coil, Nova Medical System, Wilmington, Del, USA). For fast spin echo (FSE) T_2-weighted MR imaging, the following parameters were adopted: repetition time (ms/echo) time milliseconds of 4,800/102, flip angle of 90°, echo train length of 8, field of view of 6 cm, section thickness of 2 mm, intersection gap of 0.1 mm, and 256×160 matrix.

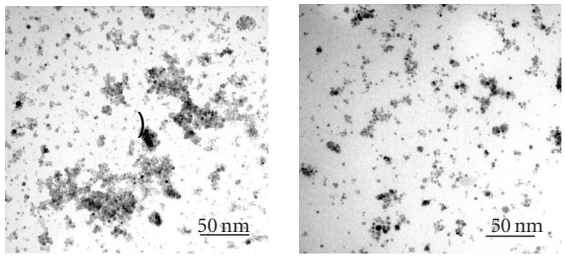

(a) (b)

Figure 4: Transmission electron micrograph of 2-pyrrolidone-coated SPIONs (a), PVLA-coated SPIONs (b).

The quantitative analysis was performed by one radiologist for MR imaging. The signal intensity (SI) was measured in defined regions of interest (ROI) in identical site of liver before (SI pre of liver) and after (SI post of liver) contrast injection. In addition, the SI in the ROI of back muscle adjacent to the liver was measured before (SI pre of BM) and after (SI post of BM). SI of back muscle is not affected by the SPIONs injection. Relative signal enhancement of liver was calculated by using the formula [(SI post of liver/SI post of BM–SI pre of liver/SI pre of BM)/SI post of liver/SI post of BM] $\times 100$.

3. RESULTS AND DISCUSSION

3.1. Preparation and characterization of PVLA-coated SPIONs

Surface modification of iron oxide nanoparticles with biocompatible polymers is potentially beneficial to prepare MRI contrast agents for in vivo applications. In particular, targeted delivering, nonaggregating, and nontoxic properties are required for the nanoparticles to achieve the accumulation in liver. To produce well-dispersed iron oxide colloidal solutions with hepatocytes targeting properties, we prepared SPIONs coated with PVLA having galactose residues as hepatocyte-specific ligand and serving as an emulsifier due to its amphiphilic property [22]. The parent nanoparticles were synthesized by coprecipitation of ferrous and ferric ions in an aqueous solution upon addition of ammonium hydroxide. Common problems of the naked magnetic nanoparticles are their tendency to agglomerate once formed and their chemical instability with respect to oxidation in air [25]. The final iron oxide compositions are very often intermediate between magnetite (Fe_3O_4) and maghemite (γ-Fe_2O_3), due to the oxidation of the particles during the synthesis [31]. The problem of oxidation-sensitive magnetite could be overcome by the deliberate introduction of a second oxidation step [25]. Stable ferrofluids for liver targeting can be prepared by adsorption of PVLA on the surface of magnetic nanoparticles after the second oxidation step. Polymer can be adsorbed by electrostatic, covalent, hydrophobic, and hydrogen bonding mechanism [32]. Hydrogen bonding is assumed to be the predominant mechanism for the adsorption of nonionic polymer such as PVLA on oxide surface. The hydrogen bonding result from the interaction between polar functional groups of PVLA and hydroxylated and protonated surface sides of the oxide [25]. The importance of surface hydroxyl functions in hydrogen bonding has been further verified by adsorbing the polymer onto pure gold sol, the surface of which is not oxidized and, therefore, dose not carry any hydroxyl groups; in this case, no adsorption of the polymer is detected [33]. Accordingly, it is believed that the hydrogen bonding may be strengthened by the second oxidation step mentioned above.

FTIR analysis was performed to confirm the coating on SPIONs surface with PVLA. Figure 2 shows a comparison between the FTIR spectra of the SPIONs (a) the pure PVLA itself (b), and the PVLA-coated SPIONs (c). The presence of magnetic iron oxide nanoparticles can be seen by two strong absorption bands at around 631 and 564 cm^{-1}. These bands result from split of the ν_1 band at 570 cm^{-1}, which corresponds to the Fe–O bond of bulk magnetite [34]. Furthermore, an adsorption band was observed at around 434 cm^{-1}, which corresponds to the shifting of the ν_2 band of the Fe–O bond of bulk magnetite (at 375 cm^{-1}) to a higher wave number [34]. The strong band at 1078 cm^{-1} as shown in the FTIR spectrum of PVLA (b) is attributed to the skeletal vibrations and C−O stretch of oligosaccharide [35], and the band at 2926 cm^{-1} and a pair of bands at 1542 and 1423 cm^{-1} are attributed to the stretch of $-CH_2$ and aromatic C=C of polystyrene backbone, respectively [12, 36]. In addition, the N−H bending and C=O stretching bands are overlapped at 1647 cm^{-1} [37]. Comparing the FTIR spectrum of SPIONs (a) and that of PVLA-coated SPIONs (c), the characteristic bands resulted from the oligosaccharide and polystyrene containing PVLA appeared near 2926 and 1078 cm^{-1}, respectively, for PVLA-coated SPIONs, indicating that PVLA was coated at the nanoparticle surface. After the adsorption of PVLA, the characteristic bands of Fe–O bond of bulk magnetite (631 and 564 cm^{-1}) shifted to the higher wave numbers of about 636 and 588 cm^{-1}, an indication of the occurrence of hydrogen bonding between hydroxyl groups of PVLA and hydroxylated and protonated surface sides of the oxide.

We compared the structure, size, and uniformity of the PVLA-coated SPIONs with those of the 2-pyrrolidone-coated SPIONs prepared for use as a control.

Figure 3 shows the XRD patterns for the 2-pyrrolidone-coated and PVLA-coated SPIONs. Six characteristic peaks (2θ = 30.1, 35.5, 43.1, 53.4, 57.0, and 62.6°), marked by their indices [(220), (311), (400), (422), (511), and (440)], were observed for 2-pyrrolidone-coated SPION samples. The positions and relative intensities of all diffraction peaks in Figure 3(a) match well with those from the JCPDS file (PCPDFWIN v.2.02, PDF No. 85-1436) for magnetite and reveal that the resultant nanoparticles were pure magnetite with spinal structure [11]. As shown in Figure 3(b), the XRD pattern of PVLA-coated SPIONs also proved its highly crystalline nature and the peaks are consistent with standard maghemite reflections [38, Supporting Information], being an indication of the magnetite-maghemite transformation due to second oxidation step. It is already known that magnetite is transformed to maghemite at pH 2 upon addition of ferric ions. Jolivet and Tronc have reported on the

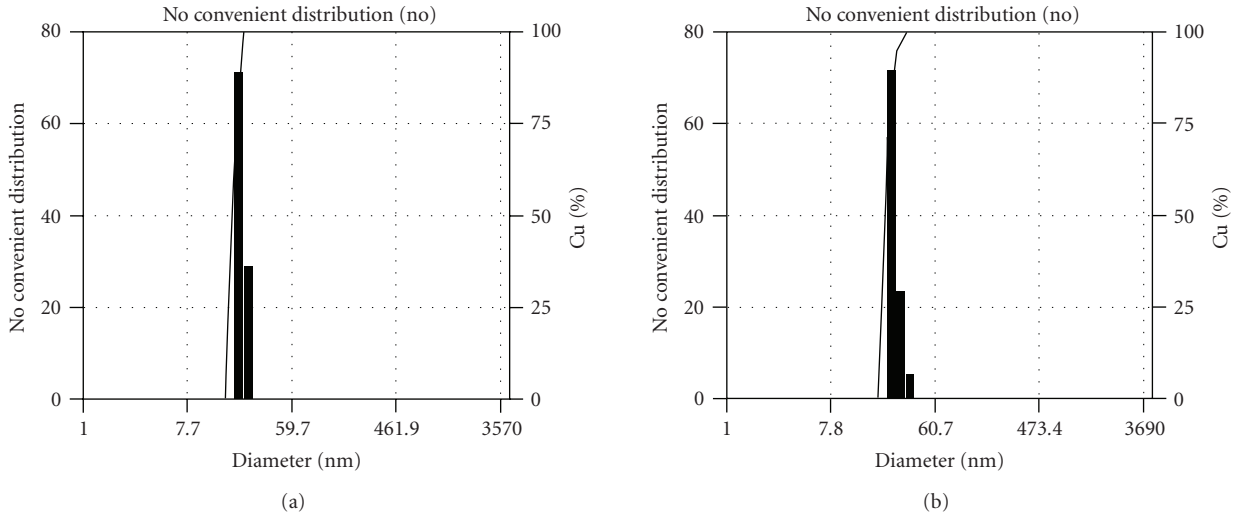

Figure 5: Particle size distribution profiles of 2-pyrrolidone-coated SPIONs (a), PVLA-coated SPIONs (b).

behavior of colloidal magnetite in acidic medium in the presence of iron nitrate and studied the phenomena that induce the magnetite-maghemite transformation [25, 39]. Further, XRD confirmed the high degree of crystallinity of the both types of particles.

The shape, size, and uniformity of the 2-pyrrolidone-coated and PVLA-coated SPIONs were observed by means of TEM. The TEM images of these both particles show ellipsoidal iron oxide particles with an average size less than 10 nm as shown in Figure 4. As well known, a representative TEM image of naked magnetic nanoparticles showed that the particles strongly agglomerated [6, 25]. On the other hand, our samples that were obtained after monomer or polymer coating reveal well-separated particles. Especially, in PVLA-coated particles (b), the particle distribution is more homogeneous than the 2-pyrrolidone-coated particles (a).

Figure 5 shows number average sizes and size distribution of synthesized magnetite and PVLA-coated SPIONs by ELS. It was clear that size distributions of both the 2-pyrrolidone-coated and PVLA-coated SPIONs were unimodal and particles were uniformly prepared. The average particle sizes were 20.8 ± 4.4 and 25.8 ± 6.1 nm for 2-pyrrolidone-coated and PVLA-coated SPIONs, respectively. The average diameters obtained by ELS were larger than the sizes determined from the TEM image for corresponding samples. This may presumably be because ELS gives a mean hydrodynamic diameter of magnetic nanoparticles surrounded by PVLA layer in aqueous solution whereas TEM gives the diameter of magnetic nanoparticles alone in dry state [40].

3.2. Observation of confocal laser scanning micrographs

The FITC on the nanoparticles allowed direct visualization of the nanoparticle uptakes into cells. Figure 6 shows fluorescence (a) and phasecontrast (b) micrographs of hepatocytes cultured in medium containing SPIONs coated with FITC-labeled PVLA according to treatment time. The fluorescence micrograph demonstrates a time-dependent uptake of FITC-PVLA-coated SPIONs into hepatocytes as shown in Figure 6(a). A significant uptake of the nanoparticles was clearly observed after 1 hour of culture. We performed a quantitative evaluation of uptake in the in vivo although only qualitative evaluation was performed in the in vitro, because the specific interaction between galactose moieties of PVLA and asialoglycoprotein receptors in the hepatocytes has been already reported.

It was also checked whether the PVLA-coated SPIONs existed in the cytosol or was only attached to the plasma membrane of hepatocyte. The cell was sectioned at various depths from cell surface by confocal laser scanning microscopy, and each fluorescence distribution was observed (see Figure 7). Fluorescence of the magnetic nanoparticles was observed more intensively inside the cell membrane and uniformly distributed in the cytosol. These results suggest that the many nanoparticles were internalized in the cytosol through a receptor-mediated endocytosis. The affinity of ASGPR to natural and synthetic oligosaccharides having nonreducing galactose residues had been reported by Lee et al. [17].

3.3. In vivo MR imaging of liver

We examined an applicability of the PVLA-coated SPIONs for in vivo liver imaging based on a T_2–weighted FSE echo imaging, which is a useful way to the liver accumulation of the magnetic nanoparticles [14]. We examined three rats to obtain the preliminary data. Liver signal intensity of all animals showed similar degree of signal drop. We described the typical case in our experiment. However, we did not calculate the statistical analysis due to small number of animals.

At 1 hour postinjection of the PVLA-coated SPIO, signal intensity of liver was hypointense compared to SI of back muscle FSE T_2-weighted MR image (data not shown). The relative signal enhancement on the FSE T_2-weighted

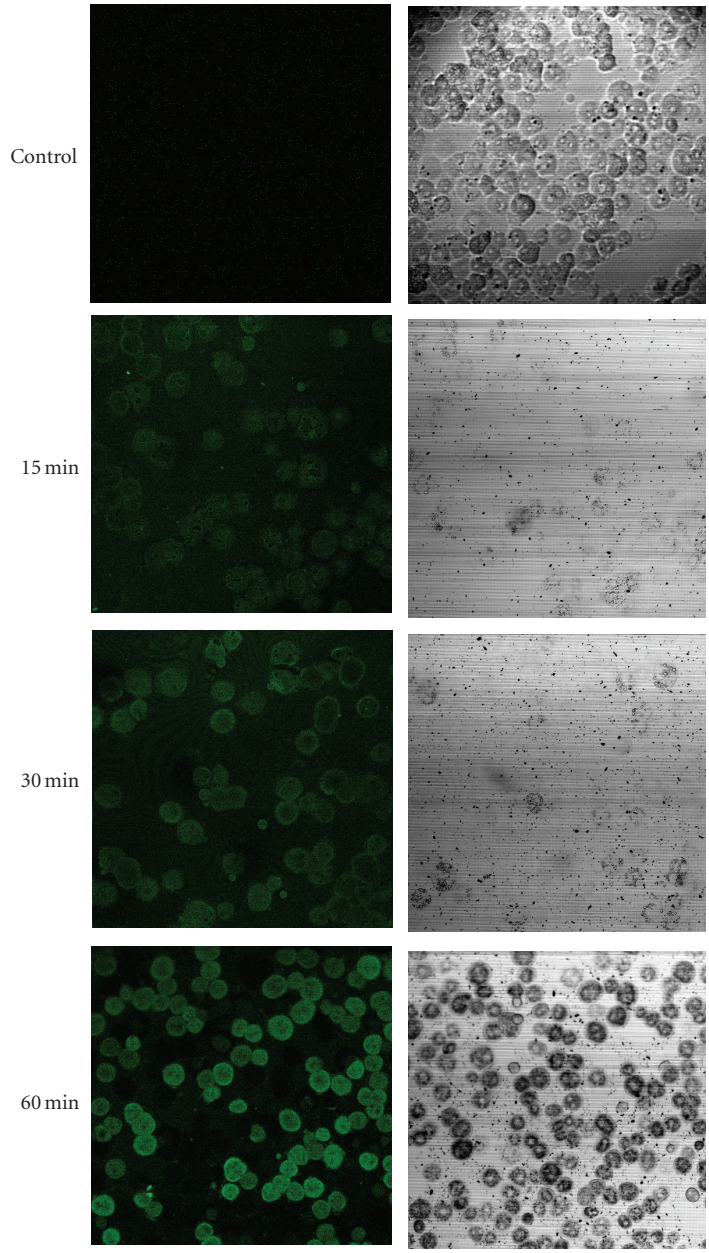

Figure 6: Fluorescence (a) and phase-contrast (b) microphotographs of hepatocytes incubated with FITC-PVLA-coated SPIONs (1 mg/mL) against time at 37°C.

MR image was observed in the liver with a T_2 signal drop of 70.9% for PVLA-coated SPIO, indication of the accumulation of nanoparticle in liver. Figure 8 shows the T_2-weighted MR images of middle part of liver before and after injection of SPIONs through tail vein. After injection of the PVLA-coated SPIONs, the SI of liver clearly dropped on T_2-weighted MR image. The relative signal enhancement of the T_2-weighted MR image was observed in the liver with a T_2 signal drop of 75.4% for PVLA-coated SPIONs and 36% for pyrrolidone-coated SPIONs. SI of liver on T_2-weighted MR image after injection of PVLA-coated SPIONs was darker than that after pyrrolidone-coated SPIONs (see Figures 8(b) and 8(d)). Thus, PVLA-coated SPIONs were more successfully targeted the liver than pyrrolidone-coated SPIONs. PVLA-coated SPIONs can be used as the hepatocyte targeted contrast agent such as mangafodipir trisodium, formerly known as Mn-DPDP [41]. Additionally, we observed accumulation in kidneys after injection of PVLA-coated SPIONs (data not shown). We think that the nanoparticles will be cleared from kidney. Renal excretion of nanoparticles is beneficial to develop nontoxic MR nanoparticles in the clinical use.

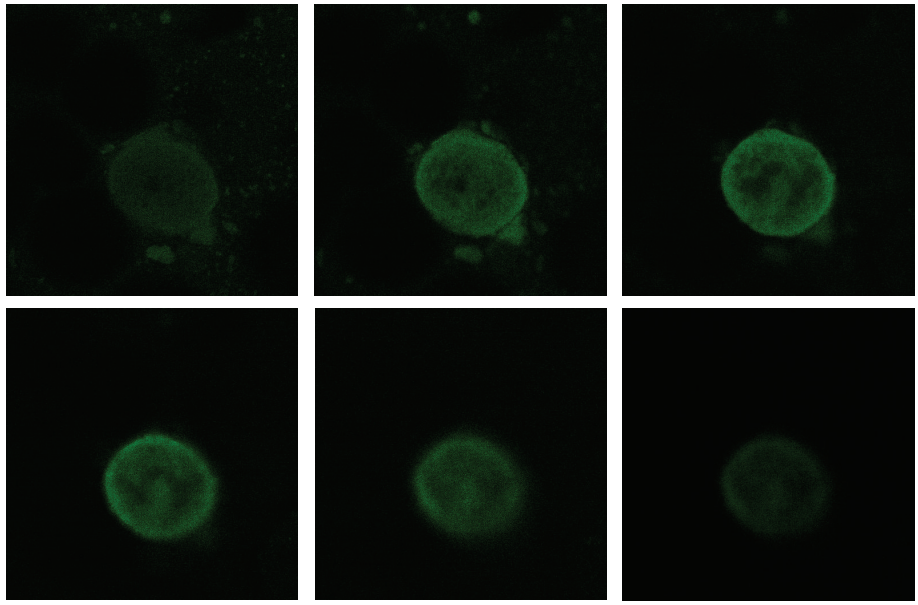

Figure 7: Confocal laser micrograph of hepatocytes incubated with FITC-PVLA coated SPIONs (1 mg/mL) for 1 hour (gallery mode observation).

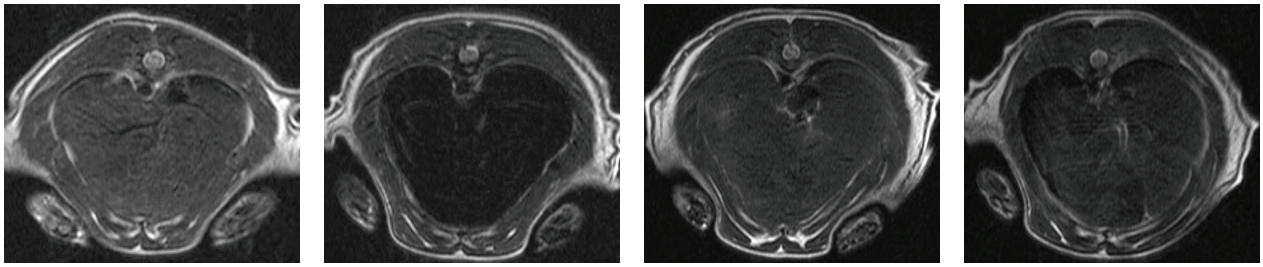

(a) (b) (c) (d)

Figure 8: T_2-weighted MR image (b) after 1-hour injection of PVLA-coated SPIONs shows marked signal drop (darkening) of liver compared to T_2-weighted MR image of preinjection (a). Degree of signal drop is mild between T_2-weighted MR image of pre- (c) and postinjection (d) of pyrroridone-coated SPIONs.

4. CONCLUSION

We have demonstrated that PVLA can serve as the coating material for SPIONs to achieve the stabilization and liver-specific delivery of ferrofluid. The PVLA-coated SPIONs of about 10 nm diameter having a core–shell structure with magnetic core and polymeric shell have been successfully prepared. The FTIR experimental results proved that the PVLA is adsorbed onto the surface of SPIONs through the hydrogen bonding between polar functional alcohol groups of PVLA and hydroxylated and protonated surface sides of the oxide. Hence the resultant nanoparticles possess an excellent solubility and stability in ferrofluid. In vivo experimental result indicated that the PVLA-coated SPIONs were accumulated in liver appreciably. Therefore, PVLA as a coating material not only prevented the aggregation between SPIONs in physiological medium but also provided a capacity to be delivered in liver specifically, which suggests the potential utility of PVLA-coated SPIONs as a contrast agent for liver diagnosis.

ACKNOWLEDGMENTS

This research was supported by a fund provided by the Ministry of Science and Technology of Korea (M10414030002-05N1403-00210). The authors also acknowledge National Instrumentaion Center for Environmental Management for permission to take ELS, FTIR, TEM, and confocal microscopy. M. K. Yoo was supported by the Brain Korea 21 Project.

REFERENCES

[1] A. K. Gupta and M. Gupta, "Synthesis and surface engineering of iron oxide nanoparticles for biomedical applications," *Biomaterials*, vol. 26, no. 18, pp. 3995–4021, 2005.

[2] R. Weissleder, A. Bogdanov, E. A. Neuwelt, and M. Papisov, "Long circulating iron oxides for MR imaging," *Advanced Drug Delivery Review*, vol. 16, no. 2-3, pp. 321–334, 1995.

[3] L. Babes, B. Denizot, G. Tanguy, J. J. Le Jeune, and P. Jallet, "Synthesis of iron oxide nanoparticles used as MRI contrast

agents: a parametric study," *Journal of Colloid and Interface Science*, vol. 212, no. 2, pp. 474–482, 1999.

[4] C. Chouly, D. Pouliquen, I. Lucet, J. J. Jeune, and P. Jallet, "Development of superparamagnetic nanoparticles for MRI: effect of particle size, charge and surface nature on biodistribution," *Journal of Microencapsulation*, vol. 13, no. 3, pp. 245–255, 1996.

[5] Y.-X. J. Wang, S. M. Hussain, and G. P. Krestin, "Superparamagnetic iron oxide contrast agents: physicochemical characteristics and applications in MR imaging," *European Radiology*, vol. 11, no. 11, pp. 2319–2331, 2001.

[6] C.-L. Lin, C.-F. Lee, and W.-Y. Chiu, "Preparation and properties of poly(acrylic acid) oligomer stabilized superparamagnetic ferrofluid," *Journal of Colloid and Interface Science*, vol. 291, no. 2, pp. 411–420, 2005.

[7] Y. Zhang, N. Kohler, and M. Zhang, "Surface modification of superparamagnetic magnetite nanoparticles and their intracellular uptake," *Biomaterials*, vol. 23, no. 7, pp. 1553–1561, 2002.

[8] A. Petri-Fink, M. Chastellain, L. Juillerat-Jeanneret, A. Ferrari, and H. Hofmann, "Development of functionalized superparamagnetic iron oxide nanoparticles for interaction with human cancer cells," *Biomaterials*, vol. 26, no. 15, pp. 2685–2694, 2005.

[9] A. J. M. D'Souza, R. L. Schowen, and E. M. Topp, "Polyvinylpyrrolidone-drug conjugate: synthesis and release mechanism," *Journal of Controlled Release*, vol. 94, no. 1, pp. 91–100, 2004.

[10] C. C. Berry, S. Wells, S. Charles, G. Aitchison, and A. S. G. Curtis, "Cell response to dextran-derivatised iron oxide nanoparticles post internalisation," *Biomaterials*, vol. 25, no. 23, pp. 5405–5413, 2004.

[11] Y.-C. Chang and D.-H. Chen, "Preparation and adsorption properties of monodisperse chitosan-bound Fe_3O_4 magnetic nanoparticles for removal of Cu(II) ions," *Journal of Colloid and Interface Science*, vol. 283, no. 2, pp. 446–451, 2005.

[12] A. K. Gupta and M. Gupta, "Cytotoxicity suppression and cellular uptake enhancement of surface modified magnetic nanoparticles," *Biomaterials*, vol. 26, no. 13, pp. 1565–1573, 2005.

[13] I. Raynal, P. Prigent, S. Peyramaure, A. Najid, C. Rebuzzi, and C. Corot, "Macrophage endocytosis of superparamagnetic iron oxide nanoparticles: mechanisms and comparison of ferumoxides and ferumoxtran-10," *Investigative Radiology*, vol. 39, no. 1, pp. 56–63, 2004.

[14] M. Kumagai, Y. Imai, T. Nakamura, et al., "Iron hydroxide nanoparticles coated with poly(ethylene glycol)-poly(aspartic acid) block copolymer as novel magnetic resonance contrast agents for in vivo cancer imaging," *Colloids and Surfaces B*, vol. 56, no. 1-2, pp. 174–181, 2007.

[15] H. Choi, S. R. Choi, R. Zhou, H. F. Kung, and I.-W. Chen, "Iron oxide nanoparticles as magnetic resonance contrast agent for tumor imaging via folate receptor-targeted delivery," *Academic Radiology*, vol. 11, no. 9, pp. 996–1004, 2004.

[16] A. Moore, J. P. Basilion, E. A. Chiocca, and R. Weissleder, "Measuring transferrin receptor gene expression by NMR imaging," *Biochimica et Biophysica Acta*, vol. 1402, no. 3, pp. 239–249, 1998.

[17] R. T. Lee, R. W. Myers, and Y. C. Lee, "Further studies on the binding characteristics of rabbit liver galactose/N-acetylgalactosamine-specific lectin," *Biochemistry*, vol. 21, no. 24, pp. 6292–6298, 1982.

[18] S.-J. Seo, H.-S. Moon, D.-D. Guo, S.-H. Kim, T. Akaike, and C. S. Cho, "Receptor-mediated delivery of all-*trans*-retinoic acid (ATRA) to hepatocytes from ATRA-loaded poly(*N*-*P*-vinylbenzyl-4-*o*-β-D-galactopyranosyl-D-gluconamide) nanoparticles," *Materials Science and Engineering C*, vol. 26, no. 1, pp. 136–141, 2006.

[19] C. S. Cho, S. J. Seo, I. K. Park, et al., "Galactose-carrying polymers as extracellular matrices for liver tissue engineering," *Biomaterials*, vol. 27, no. 4, pp. 576–585, 2006.

[20] R. L. Hudgin, W. E. Pricer Jr., G. Ashwell, R. J. Stockert, and A. G. Morell, "The isolation and properties of a rabbit liver binding protein specific for asialoglycoproteins," *Journal of Biological Chemistry*, vol. 249, no. 17, pp. 5536–5543, 1974.

[21] S. Hirose, H. Ise, M. Uchiyama, C. S. Cho, and T. Akaike, "Regulation of asialoglycoprotein receptor expression in the proliferative state of hepatocytes," *Biochemical and Biophysical Research Communications*, vol. 287, no. 3, pp. 675–681, 2001.

[22] A. Maruyama, T. Ishihara, N. Adachi, and T. Akaike, "Preparation of nanoparticles bearing high density carbohydrate chains using carbohydrate-carrying polymers as emulsifier," *Biomaterials*, vol. 15, no. 13, pp. 1035–1042, 1994.

[23] K. Kobayashi, H. Sumitomo, and Y. Ina, "Synthesis and functions of polystyrene derivatives having pendent oligo sacharides," *Polymer Journal*, vol. 17, no. 4, pp. 567–575, 1985.

[24] G. A. Van Ewijk, G. J. Vroege, and A. P. Philipse, "Convenient preparation methods for magnetic colloids," *Journal of Magnetism and Magnetic Materials*, vol. 201, no. 1–3, pp. 31–33, 1999.

[25] M. Chastellain, A. Petri, and H. Hofmann, "Particle size investigations of a multistep synthesis of PVA coated superparamagnetic nanoparticles," *Journal of Colloid and Interface Science*, vol. 278, no. 2, pp. 353–360, 2004.

[26] X. Hong, W. Guo, H. Yuan, et al., "Periodate oxidation of nanoscaled magnetic dextran composites," *Journal of Magnetism and Magnetic Materials*, vol. 269, no. 1, pp. 95–100, 2004.

[27] Z. Li, H. Chen, H. Bao, and M. Gao, "One-pot reaction to synthesize water-soluble magnetic nanocrystals," *Chemistry of Materials*, vol. 16, no. 8, pp. 1391–1393, 2004.

[28] P. O. Seglen, "Preparation of isolated rat liver cell," *Methods in Cell Bioloy*, vol. 13, pp. 29–83, 1976.

[29] M. Aubele, H. Zitzelsberger, S. Szücs, et al., "Comparative FISH analysis of numerical chromosome 7 abnormalities in 5-μm and 15-μm paraffin-embedded tissue sections from prostatic carcinoma," *Histochemistry and Cell Biology*, vol. 107, no. 2, pp. 121–126, 1997.

[30] C. S. Cho, A. Kobayashi, R. Takei, T. Ishihara, A. Maruyama, and T. Akaike, "Receptor-mediated cell modulator delivery to hepatocyte using nanoparticles coated with carbohydrate-carrying polymers," *Biomaterials*, vol. 22, no. 1, pp. 45–51, 2001.

[31] C. Cannas, D. Gatteschi, A. Musinu, G. Piccaluga, and C. Sangregorio, "Structural and magnetic properties of Fe_2O_3 nanoparticles dispersed over a silica matrix," *Journal of Physical Chemistry B*, vol. 102, no. 40, pp. 7721–7726, 1998.

[32] D. H. Napper, *Polymeric Stabilisation of Colloidal Dispersions*, Academic Press, New York, NY, USA, 1983.

[33] L. T. Lee and P. Somasundaran, "Adsorption of polyacrylamide on oxide minerals," *Langmuir*, vol. 5, no. 3, pp. 854–860, 1989.

[34] M. Yamaura, R. L. Camilo, L. C. Sampaio, M. A. Macêdo, M. Nakamura, and H. E. Toma, "Preparation and characterization of (3-aminopropyl)triethoxysilane-coated magnetite nanoparticles," *Journal of Magnetism and Magnetic Materials*, vol. 279, no. 2-3, pp. 210–217, 2004.

[35] C. V. Luyen and D. M. Huong, "Chitin and derivatives," in *Polymeric Materials Encyclopedia*, J. C. Salomone, Ed., vol. 2, pp. 1208–1217, CRC Press, Boca Raton, Fla, USA, 1996.

[36] P. Galgali, M. Agashe, and A. J. Varma, "Sugar-linked biodegradable polymers: regio-specific ester bonds of glucose hydroxyls in their reaction with maleic anhydride functionalized polystyrene and elucidation of the polymer structures formed," *Carbohydrate Polymers*, vol. 67, no. 4, pp. 576–585, 2007.

[37] Y.-C. Chang, S.-W. Chang, and D.-H. Chen, "Magnetic chitosan nanoparticles: studies on chitosan binding and adsorption of Co(II) ions," *Reactive and Functional Polymers*, vol. 66, no. 3, pp. 335–341, 2006.

[38] T. H. Hyeon, S. S. Lee, J. N. Park, Y. H. Chung, and H. B. Na, "Synthesis of highly crystalline and monodisperse maghemite nanocrystallites without a size-selection process," *Journal of the American Chemical Society*, vol. 123, no. 51, pp. 12798–12801, 2001.

[39] J. P. Jolivet and E. Tronc, "Interfacial electron transfer in colloidal spinel iron oxide. Conversion of Fe_3O_4-γ-Fe_2O_3 in aqueous medium," *Journal of Colloid and Interface Science*, vol. 125, no. 2, pp. 688–701, 1988.

[40] K. M. Kamruzzaman Selim, Y.-S. Ha, S.-J. Kim, et al., "Surface modification of magnetite nanoparticles using lactobionic acid and their interaction with hepatocytes," *Biomaterials*, vol. 28, no. 4, pp. 710–716, 2007.

[41] U. Kettritz, J. F. Schlund, K. Wilbur, L. B. Eisenberg, and R. C. Semelka, "Comparison of gadolinium with manganese-DPDP of liver lesion detection and characterization: preliminary results," *Magnetic Resonance Imaging*, vol. 14, no. 10, pp. 1185–1190, 1996.